

● Porous Anionic Co(II) Metal-Organic Framework, with a High Density of Amino Groups, as a Superior Luminescent Sensor for Turn-on Al(III) Detection

Santanu Chand,^[a] Gaurav Verma,^[b] Arun Pal,^[a] Shyam Chand Pal,^[a] Shengqian Ma,^[b] and Madhab C. Das^{*[a]}

Dedicated to Dr. Subhadip Neogi.

Abstract: Accumulation of high concentrations of Al(III) in body has a direct impact on health and therefore, the trace detection of Al(III) has been a matter for substantial concern. An anionic metal organic framework ($\{[Me_2NH_2]_{0.5}[Co(DATRz)_{0.5}(NH_2BDC)] \cdot xG\}_n$; 1; HDATRz = 3,5-diamino-1,2,4-triazole, H_2NH_2 -BDC = 2-amino-1,4-benzenedicarboxylic acid, G = guest molecule) composed of two types of secondary building units (SBU) and channels of varying sizes was synthesized by employing a rational design mixed ligand synthesis approach. Free $-NH_2$ groups on both the ligands are immobilized onto the pore surface of the MOF which acts as a superior luminescent sensor for turn-on Al(III) detection. Furthermore, the large channels could allow the counter-ions to pass through and get exchanged to selectively detect Al(III) in presence of other seventeen metal ions with magnificent luminescence enhancement. The observed limit of detection is as low as 17.5 ppb, which is the lowest among the MOF-based sensors achieved so far. To make this detection approach simple, portable and economic, we demonstrate MOF filter paper test for real time naked eye observation.

Aluminum is the most widespread element after oxygen and silicon and the most abundant metal ion in the biosphere.^[1] While pure aluminum does not occur naturally, the frequent usage in human activities causes Al(III) ions to release in the environment. The gradual gathering of Al(III) in human body with a high dose directly influences nervous system, causing many symptoms of Al(III) toxicity for instance Alzheimer's


disease, Parkinson's syndrome and osteoporosis.^[2] According to the WHO guidelines, a provisional tolerable weekly intake (PTWI) for aluminium from all sources is 1 mg/kg of body weight.^[3] The practicable levels of aluminium in large and small drinking-water plants using aluminium-based coagulants are ≤ 0.1 mg/L and ≤ 0.2 mg/L, respectively.^[3] Therefore, it is crucial to foster new materials capable of detecting exclusively trace amount of Al(III) in presence of other metal ions without requirement of expensive instrumentations.

Although, traditional organic luminescent sensors for Al(III) detection are reported, they suffer from limitations such as long response time, multi-step synthesis process, non-recyclability, and rapid interference with other metal ions.^[4] On the other hand, an increasing number of luminescent metal-organic frameworks (LMOFs) have been reported showing great promise as effective luminescence sensors for small molecules, metal cations, anions and protons.^[5] In particular, Chen and coworkers pioneered the works on LMOFs for Cu^{2+} ions and small molecules sensing through luminescence quenching by introducing special functional sites onto the framework backbone.^[6] In contrast, the development of LMOFs as Al(III) sensors is still in its infancy^[7] particularly in terms of designing strategies leading to super selectivity and ultrahigh sensitivity. From an economic perspective and possible widespread practices, the transition-metals-based LMOF probes for Al(III) sensing are highly desirable together with luminescence 'turn-on' sensing display. Such 'turn-on' display could preclude the wrong response with a higher signal-to-noise in the dark background.^[8]

The mixed-ligand synthesis approach through judicious choice and successful combination of various types of acid-acid and acid-base ligands has directed the construction of MOFs with impressive structures, enhanced tunability and remarkable properties.^[9–10] In recent years, the research on LMOFs highlighted the significant role of binding sites within the porous frameworks, such as Lewis basic unbound pyridyl group, uncoordinated $-NH_2$ and $-OH$ groups to enhance unique recognition and selective detection of different metal ions.^[6a,11] In all such cases, a single organic ligand was used bearing either of those functional sites to construct the targeted LMOF.^[6a,11] The mixed ligand strategy also has shown its effectiveness to construct a handful of porous LMOF-based metal ion sensors but the binding sites are placed on either of the two ligands.^[7a–c,12] In order to boost the selectivity and sensitivity (to achieve lower limit of detection, LOD) towards a particular

[a] S. Chand, A. Pal, S. C. Pal, Dr. M. C. Das
Department of Chemistry
Indian Institute of Technology Kharagpur
Kharagpur-721302, WB (India)
E-mail: mcdas@chem.iitkgp.ac.in
Homepage: <https://www.chemiitkgp-mcdaslab.com/>

[b] G. Verma, Prof. S. Ma
Department of Chemistry
University of North Texas
Denton, TX 76201 (USA)

 Supporting information for this article is available on the WWW under <https://doi.org/10.1002/chem.202101692>

metal ion, it would be appropriate to immobilize plentiful free binding sites onto the MOF backbone and the mixed ligand strategy may readily fulfill this criteria when both the constituent ligands are decorated with binding sites. To the best of our knowledge, this concept has never been realized to construct LMOF probes for metal ion sensing.

In order to facilitate the pre-concentration of the analytes into the LMOF pores, two separate strategies have been employed so far: i) immobilization of free binding sites as discussed^[6a,7a-c,11] or ii) cation exchange approach^[7d,13] where exchangeable counter cations in the pores are replaced by targeted metal ion for sensing application. We hypothesized that combination of both the strategies would eventually induce a synergistic effect between the two to achieve the highest selectivity and lowest detection limit. However, these two strategies have never been exploited together. Additionally, crystallographic identification of counter-cations into the pores could benefit in gaining a better insight into the structure-function relationship which are often too disordered and are excluded from Difference Fourier Map.

Bearing the aforementioned facts in mind, herein, we have chosen two ligands: HDATRz (3,5-diamino-1,2,4-triazole) and H₂NH₂-BDC (2-amino-1,4-benzenedicarboxylic acid) having plentiful free -NH₂ binding sites on both ligands to construct a highly porous 3D Co(II)-MOF (**1**) with molecular formula $\{[Me_2NH_2]_{0.5}[Co(DATRz)_{0.5}(NH_2BDC)] \cdot xG\}_n$ (G = guest molecule) by employing the mixed ligand strategy. This Co(II)-MOF is anionic with exchangeable counter cations in the pores. Strikingly, its luminescence can be selectively and solely enhanced by a trace amount of Al(III) ions with LOD 17.5 ppb which is the lowest among MOF-based Al(III) sensors.

The accumulation of triangular ligand HDATRz, linear H₂NH₂-BDC, and cobalt(II) dimers leads to the formation of new anionic amino-decorated MOF (**1**) in high yield as deep violet rectangular crystals via solvothermal synthesis. **1** crystallizes in the high symmetric tetragonal crystal system with space group *P4₂/nnm*. There are two independent Co(II) ions with half occupancy, one NH₂-BDC²⁻ ion, half of the triangular DATRz⁻ and half of the cationic guest in the asymmetric unit (Figure S1, Supporting Information). The cationic guests are generated in situ from the decomposition of DMF and could be located in the channels from Difference Fourier Map to balance the overall charge. Among the two different Co(II) ions, one is coordinated by four O atoms from four NH₂-BDC ligands and one N atom from the DATRz unit at the vertex resulting in a five coordinated square pyramidal paddle wheel geometry (Figure 1). The other Co(II) center is coordinated in tetrahedral fashion by two O atoms from two NH₂-BDC units and two N atoms from two DATRz units. Four carboxylate groups coordinate to two Co(2) centers, forming a [Co₂(CO₂)₄] paddle-wheel SBU (SBU1) whereas, two DATRz units join Co(1) centers together with four carboxylates to form dinuclear triazole-carboxylate SBU [Co₂(DATRz)₂(COO)₄] (SBU2, Figure S2, Supporting Information). The SBU1 and SBU2 are alternatively connected to each other running along crystallographic 'c' axis (Figure S3, Supporting Information); which are further connected by NH₂-BDC ligands to construct the highly porous 3D structure. The framework

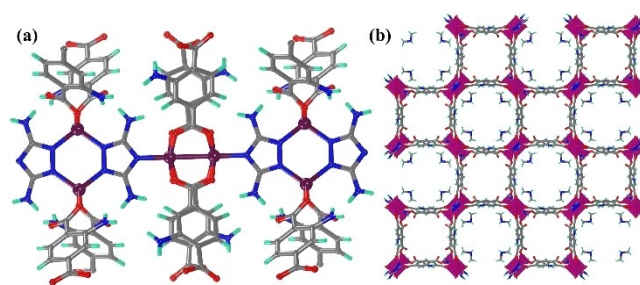


Figure 1. (a) The coordination environment around Co (II) metal centers. (b) Overall packing diagram of **1** (rectangular channels are occupied by guest Me₂NH₂⁺ cations). Color code: Co, violet; N, blue; O, red; C, grey; H, cyan.

consists of two types of channels (15.2×13.1 Å² for the rectangular channels and the tubular channel of diameter 9.2 Å considering van der Waals radii) as depicted in Figure 1b and Figure S4, Supporting Information. The counter-ions occupy rectangular channels facing the interior of the cavity from the four corners, whereas the amine groups of the NH₂-BDC moieties are pointed towards this channel from the four side arms. On the other hand, the tubular channel is decorated with amine groups of DATRz moieties from SBU2 (Figure S4, Supporting Information). The PLATON calculation without removing counter-ions indicates that this framework affords a porosity of 51.8% unit cell volume.^[14] Topologically, the framework can be simplified to a 3D uninodal, non-interpenetrating 6-connected *pcu* alpha-Po primitive cubic network (Figure S5, Supporting Information). Thermo-gravimetric analysis of **1** reveals a weight loss of 17% below 100 °C attributed to the loss of lattice solvents and the framework is thermally stable until 250 °C (Figure S6, Supporting Information).

The solid-state excitation and emission spectra of **1** and its constituting ligands are shown in Figure S7 (Supporting Information). **1** displays highly blue emissive nature centred at 430 nm while excited at 340 nm. This is attributed to the intra-ligand and ligand-to-ligand charge transfer transition (LLCT) ($\pi^* \rightarrow \pi$ and $\pi^* \rightarrow n$ transitions) of two ligands, perturbed by the coordination effect to the metal center (Figure S7, Supporting Information).^[7a,c,15] Although, luminescence compounds of transition metal ions are generally based on closed shell d¹⁰ systems, open shell Co(II) based luminescent coordination compounds are being increasingly reported.^[7a,c,g] Considering the emissive nature coupled with unique structural properties (large channels with varying sizes, highly dense uncoordinated amine groups on pore walls and exchangeable cations) it is anticipated that targeted metal cations could be diffused into the channels. This could facilitate the replacement of the encapsulated Me₂NH₂⁺ cations in rectangular channels through stronger interactions with free amines and thus rendering **1** as a potential luminescent sensor.

The luminescence property of **1** towards eighteen different metal cations has been examined (1 mM aqueous solution). The detection experiments showed that upon addition of aqueous Al(III) solution (as Al(NO₃)₃·9H₂O) into the MOF suspension in DMF (1 mg in 2 mL DMF), the luminescence intensity of the

suspension showed a significant enhancement with increasing concentration of Al(III) (Figure 2). On the other hand, all other metal ions have no obvious enhancing effect on the emission intensity under the similar experimental conditions (Figure S8–S9, Supporting Information).

The changes in luminescence intensity based on the emission at 430 nm with respect to the intensity ratio $[(I/I_0) - 1]$ values are depicted in Figure 3a as a bar diagram which clearly reveals the fact that **1** can detect Al(III) ions selectively. A nearly 4.5-fold enhancement was observed when the concentration of the aqueous solution of Al(III) reaches to 50 μL . From the calibration curve, the calculated value of LOD appears to be 0.65 μM , which is equivalent to 17.5 ppb for Al(III) ions (Figure S10, Supporting Information). To the best of our knowledge, this is the lowest LOD achieved thus far amongst MOF based sensors (Table S3, Supporting Information).

Generally, several metal ions are present in wastewater or pollutants. Therefore it is very important to examine the selectivity of **1** to Al(III) ions in the presence of several other cationic species. As depicted in Figure 3b it is clear that the emission intensity enhancement of Al(III) could still be observed in presence of all other cations, though the intensity is only slightly reduced. The luminescence intensity of **1** for a mixed ion sample (mixture of other seventeen ions) remains quenched about 15% whereas, by introducing the Al(III) in the mixture of the solution, there is a magnificent enhancing effect of the suspension (Figure 4). This consequence demonstrates that the other cations have negligible effect on the recognition of the Al(III) ions and the detection selectivity of **1** for Al(III) ions is superior even in the presence of two or more metal ions. It may be noted that the selectivity of Al(III) ion could be achieved even in the presence of the highest quenchable metal ions especially Fe(III) in contrast with those sensors exhibiting luminescence quenching both for Al(III) and Fe(III).^[16] The enhancing emission colour change upon addition of Al(III) ions could be readily visible with clear distinction while the

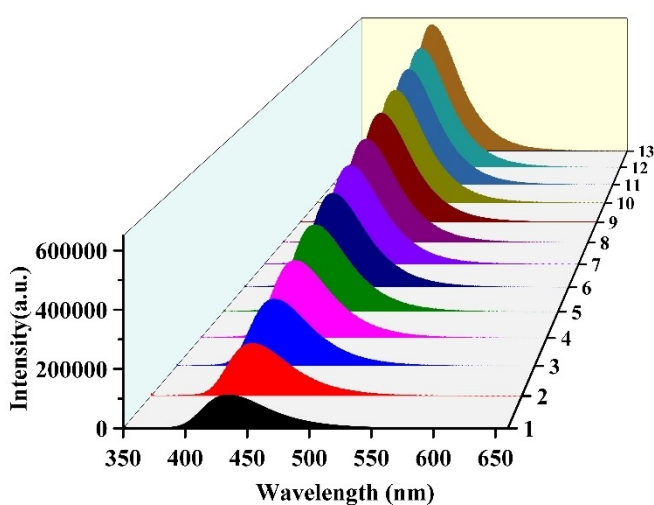


Figure 2. The emission spectra of **1** dispersed in DMF solution with increasing concentration of 1 mM Al(III) aqueous solution. The excitation wavelength was 340 nm.

suspensions are excited at 365 nm UV light (inset of Figure 4 and Figure S11, Supporting Information). We have also performed the luminescence spectra for **1** in the presence of a Lewis acid, boron trifluoride (BF_3). The luminescence intensity of the MOF suspension showed a significant enhancement with addition of BF_3 (Figure S12, Supporting Information). The observation of the luminescence intensity for **1** with BF_3 , is similar to our present study for the Al(III) detection. Furthermore, the luminescence image under 365 nm UV-light exhibited persistent bright luminescent color of the MOF suspension in presence of BF_3 while there is no effect in appearance of Fe^{3+} ions (Figure S12, Supporting Information).

The integrity of the framework is sustained with retention of crystallinity during and post-sensing experiments as evident from Powder X-ray diffraction studies (Figure S13, Supporting Information). In order to confirm the exchange process, FTIR spectrum are recorded for pristine **1** and Al(III) loaded **1**. The characteristic absorption peak at 2480 cm^{-1} for cationic Me_2NH_2^+ species in **1** disappears completely for Al(III) loaded **1**. This suggests successful exchange of Me_2NH_2^+ species with Al(III) ions.^[17] The stretching vibrations peaks for $-\text{NH}_2$ groups in Al(III) loaded **1** are significantly weaker compared to pristine **1** implying stronger interactions of $-\text{NH}_2$ groups with Al(III) (Figure S18, Supporting Information). For comparison, the luminescence properties of both the organic ligands and the mixture of these two ligands were also investigated for sensing of cations suggesting no obvious luminescence changes (Figure S19, Supporting Information). Such studies indicate that the organic ligands cannot act as luminescent sensors for Al(III).

On the other side, the photo luminescent decay dynamics of **1** before and after adding Al(III) is shown in Figure S20–21 (Supporting Information). After the immediate addition of 1 mM aqueous Al(III) solution in 2 mL dispersion of **1**, the luminescence lifetime of 723 μs in **1** is significantly enhanced to 951 μs manifesting the luminescence turn on in presence of Al(III). Our several attempts to elucidate the crystal structure of Al@**1** were unsuccessful as the single crystals became opaque and diffracted poorly after the immersion of crystals in Al(III) solutions. As anticipated, the ultrahigh selective and sensitive luminescence turn on performance of **1** towards Al(III) ions may be ascribed with the following facts: (I) high porosity of the MOF facilitates the diffusion of Al(III) into both types of channels, (ii) the abundant free amino groups of both the ligands can act as a simple electron donor to Al(III) ions through Lewis acid base type of interactions, (III) the higher charge density of Al(III) allows the frameworks stronger N–Al(III) interactions.^[18] Furthermore, to resolve the interactions between the framework and Al(III) in the pores, firstly Al(III) ions are introduced into the MOF suspension for the luminescence enhancement followed by addition of 0.1 M solution of EDTA as a masking agent. As shown in the Figure S23 (Supporting Information) the luminescence increment is not affected when the EDTA was introduced into solution. This stipulates that the Al(III) ions are strongly confined in the pores of the framework and are not loosely attached with the surface interactions. To get a better insight into the phenomenon, the energy dispersive spectroscopy

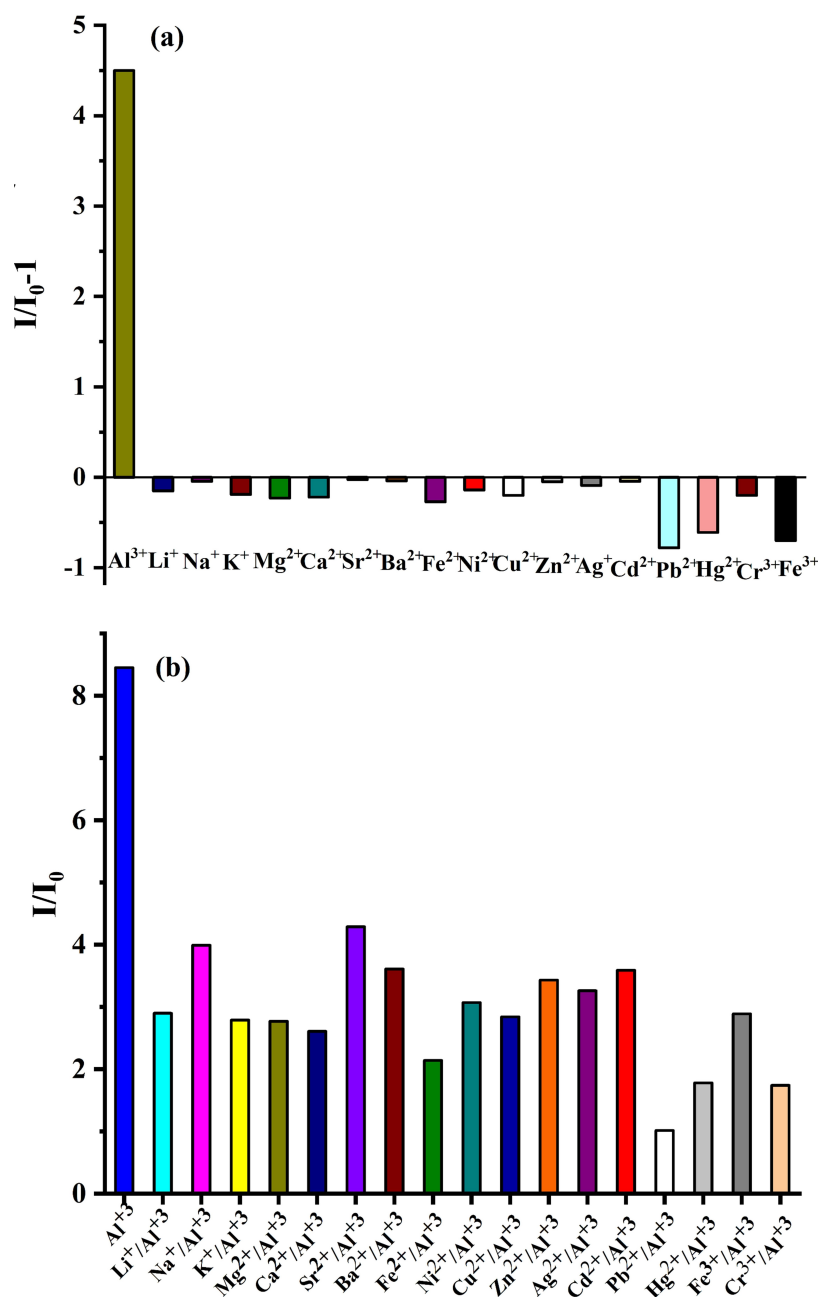


Figure 3. (a) Changes of luminescence intensity with respect the emission of 1 at 430 nm with the addition of 50 μ L of aqueous solution containing 1 mM of different metal ions. (b) The comparison of the fluorescence intensity of 1 with the addition of Al(III) and other cations (60 μ L each, 1 mM solution).

(EDS) elemental mapping of Al(III)-loaded 1 was performed after the luminescence study. As shown in Figure S24 (Supporting Information), aluminium in the sample is homogeneously allotted and indeed incorporated into the voids of 1.

To further explain the interaction between the framework and Al(III), X-ray photo electron spectroscopy (XPS) studies are carried out for both the pristine 1 and 1 after Al(III) sensing (Figure S25, Supporting Information). In contrast with 1, the N1s peak from free amine groups at 399.9 eV is shifted to 400.1 eV with the addition of Al(III) ions. This clearly demonstrates the binding of Al(III) ions to abundant amine groups into the pores

of 1. The presence of an additional peak at 406.2 eV in the N1s spectra of 1 after Al(III) sensing is ascribed to nitrate counter anion.^[6a] Moreover, the interference of different anions with altered aluminium salts (i.e., $AlCl_3$, $Al(NO_3)_3$ and $Al_2(SO_4)_3$) have been inspected; where the results disclosed that regardless of the type of Al-salts used, always there is a luminescent turn on when Al-salts is added on to the dispersed MOF suspension (Figure S26, Supporting Information). We presume that nitrate counter anions in the cavity is required to compensate the extra positive charge of exchanged tri-positive Al(III) ions with mono-positive $Me_2NH_2^+$ ions.

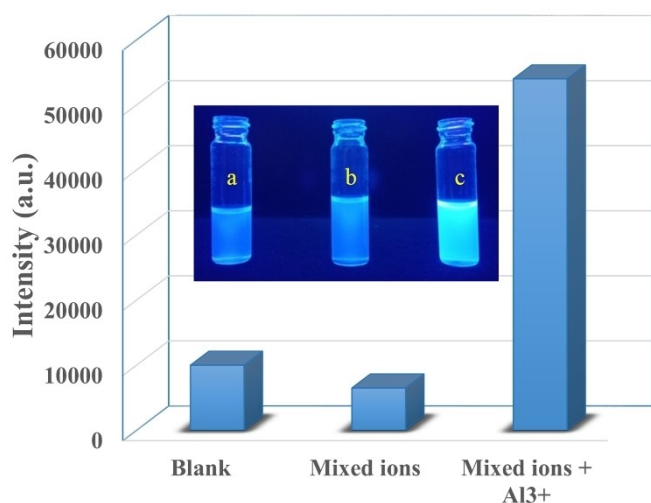


Figure 4. Comparison of the luminescence intensity of **1** under mixed metal ions. The insets are the corresponding luminescence images under 365 nm UV-light irradiation. Mixed ions refers to mixture of all seventeen metal ions other than Al(III) (equal volume of 1 mM each solution).

To investigate the probable luminescent enhancement mechanism in presence of Al(III), UV-vis absorption spectra of **1** is performed. As shown in Figure S27 (Supporting Information) after the addition of Al(III) the intensity of absorbance spectra of **1** increases significantly while in presence of all the other metal ions there is no change in intensity in the range of 330 to 380 nm. To further check the effect of metal ion itself, the UV-vis absorption spectra of all the metal ions in aqueous solution have been measured (Figure S28, Supporting Information). The results show the absence of 330 to 380 nm peak even for Al(III). Thus, the enhancement in absorbance in presence of Al(III) might be due to the complexation between **1** and Al(III), not for bare Al(III). Furthermore, the absorption spectra of the constituent ligands H₂NH₂-BDC and HDATrz after adding metal ions (Figure S29, Supporting Information) are investigated showing no apparent changes before and after addition. Hence, it may be the case that the significant absorbance enhancement of **1** with Al(III) causes the luminescence turn on due to the complexation of **1** with Al(III). We have further checked the absorption spectra of **1** after addition of different concentration of Al(III) solutions. It is observed that absorbance of **1** gradually increases with increasing concentration of Al(III) solution reminiscent to the luminescence emission enhancement phenomena (Figure S30, Supporting Information). On the basis of the above observations, absorbance caused luminescence enhancement mechanism is likely to play the role^[19] i.e., after adding Al(III) ions the electron of Al³⁺@**1** complex in the ground state can absorb more energy from the light source and then moved to the excited state followed by a series of vibrational relaxations and return of excited electrons with releasing the energy as luminescence.^[19] Al³⁺@**1** complex releases more energy during the emission process than the pristine **1** causing turn on phenomena. In general, turn-on luminescent response arises when the excited electrons transfer from a high-lying π^* -

type LUMO to the conduction band of MOF.^[5] In this consequence, the most feasible turn-on response of **1** can be interpreted as electrons transfer interactions between Al³⁺ ions and **1**. Additionally, the equilibrium adsorption uptake capacity as a function of time have been executed. The result shows a relatively low uptake and does not change much with an increase in concentration. The adsorption capacity reaches 13.5 mg/g after 20 min which remains the same up to 2 h. The measurements were extended to 8 h but the capacity does not change much. These results thus imply a minimal adsorption of Al(III) in pores and it can be assumed that Al(III) is just interacting with the MOF on the pore surfaces through charge-transfer and Lewis acid base type of interaction between Al³⁺ and -NH₂ groups. We furthermore tested the quantitative analyses of Al(III) content for the newly synthesized MOF (**2**) with less number of -NH₂ groups in it (isostructural to **1**, the number of -NH₂ groups present in **1** and **2** are two and one respectively per formula unit), by the self-assembly of HDATrz and H₂BDC (1,4-benzenedicarboxylic acid) instead of H₂NH₂-BDC present in **1**). Unfortunately, we did not get any consistent value, rather it appears as indistinct result with a large error over the time which might imply even much lower adsorption in **2**. It is noteworthy that, **2** is luminescence silent (probably because of the luminescent silent ligand systems in **2**). Even after addition of Al³⁺ solution in higher concentration the luminescent intensity is not boosted. Thus, it could be claimed that **1** could act as a superior luminescent sensor for Al(III) detection, but does not have the potential for its adsorptive removal. All such observations might be indicative of effectiveness of mixed-ligand strategy to construct LMOFs bearing abundant -NH₂ groups on both the ligands to accumulate high density of such groups onto the pore surfaces for being efficient luminescent sensors.

Recyclability with fast and simple regeneration methods is one of the key factors of a sensor for its widespread usage in real needs. It has been demonstrated that **1** can be easily recycled and reused with no loss in luminescent turn on efficiency (Figure S31, Supporting Information). **1** could also preserve its crystallinity (Figure S13, Supporting Information) at least for three consecutive cycles.

To make our detection approach simple, portable and economic, we fabricated MOF test filter paper for sensing Al(III) ions. The MOF filter papers were made effortlessly by dipping Whatman filter paper cut into ~1×6 cm strips into the DMF suspension of **1** and dried in open air for ten minutes. The detection of metal ions in aqueous solution was carried out by dripping the solutions onto the MOF test filter papers. The test filter papers showed a significant enhancement in brightness for Al(III) suggesting luminescent turn on compared to the dark color of pristine test paper under 365 nm UV-light irradiation (Figure 5). When individual ions or mixture of ions are dripped on test papers, there is no significant influence in luminescent intensity (Figure 5). Again, when an aqueous solution containing all mixed Al metal ions including Al(III) ions is dripped, test paper showed the bright luminescent colour easily distinguishable by the naked eye (Figure 5). It should be noted that concentrations to prepare test filter papers and the analytes are

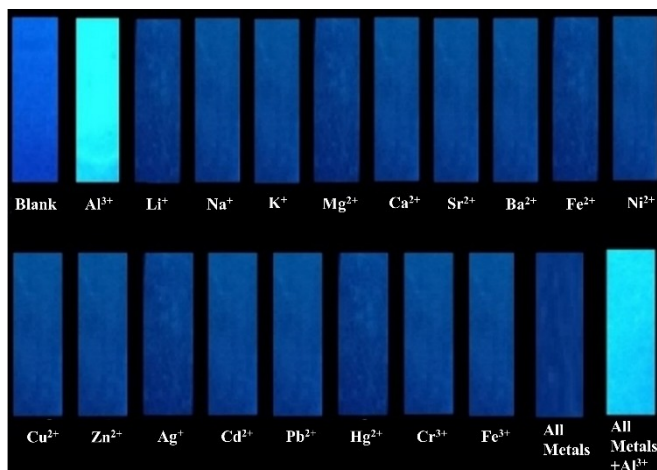


Figure 5. Photograph the MOF test filter papers after addition of different aqueous metal ions followed by exposure under 365 nm UV-light irradiation.

similar to that of the solution state studies suggesting the ability of test filter papers to sense exclusively Al(III) even for such a low level of concentration. Therefore, this method shows the potential of practical utility of 1 to act as a probe for Al(III) highlighting the simplicity and feasibility of the approach.

In conclusion, we demonstrate a general approach to achieve high performance turn-on Al(III) detection attaining the lowest LOD with a MOF-based sensor. The sensor possesses large channels and exposed abundant Lewis basic sites decorate the pore walls. The ultrahigh selectivity and sensitivity can be attributed to the synergistic effect of fast diffusion of Al(III) into the pores to get exchanged with cationic guests and enhanced binding with highly dense basic sites. The turn on sensing phenomena is rapid and selective with visual colorimetric changes under UV exposure and thus rendering the MOF as a potential real-time sensor. Immobilization of a large number of free binding sites ($-\text{NH}_2$, pyridyl N, $-\text{OH}$, amide, anionic sulfonate) onto the framework backbone to construct anionic MOFs with available design principles^[20] through mixed ligand synthesis approach could be an effective strategy to induce preferential binding with ultralow detection of targeted ions, and thus leading to the development of superior luminescent MOF probes for sensing applications in near future.

Deposition Number(s) 1913277 (for 1) and 2040381 (for 2) contain(s) the supplementary crystallographic data for this paper. These data are provided free of charge by the joint Cambridge Crystallographic Data Centre and Fachinformationszentrum Karlsruhe Access Structures service www.ccdc.cam.ac.uk/structures.

Acknowledgements

S.C. thanks IIT KGP for SRF fellowship. M.C.D. gratefully acknowledges the financial support received from SERB, New Delhi as Core Research Grant (CRG/2019/001034). S.M acknowledges the support from the US National Science Foundation (DMR-

1352065) and the Robert A. Welch Foundation (B-0027). The authors would also like to acknowledge Dr. Zachary Atlas from Geochemical Research Laboratory at the University of South Florida for ICP-OES measurements.

Conflict of Interest

The authors declare no conflict of interest.

Keywords: Aluminium · anionic · luminescence · sensors · metal-organic frameworks

- [1] a) Z. Krejpcio, R. W. P. Wojciak, *Pol. J. Environ. Stud.* **2002**, *11*, 251–254; b) J. Barceló, C. Poschenrieder, *Environ. Exp. Bot.* **2002**, *48*, 75–92.
- [2] a) G. D. Fasman, *Coord. Chem. Rev.* **1996**, *149*, 125–165; b) P. Nayak, *Environ. Res.* **2002**, *89*, 101–115; c) C. S. Cronan, W. J. Walker, P. R. Bloom, *Nature* **1986**, *324*, 140–147.
- [3] a) G. Berthon, *Coord. Chem. Rev.* **2002**, *228*, 319–341; b) FAO/WHO (1995) Pesticide residues in food-1994 evaluations WHO (2003) Aldrin and dieldrin in drinking-water.
- [4] a) M. Arduini, F. Felluga, F. Mancin, P. Rossi, P. Tecilla, U. Tonellato, N. Valentinuzzi, *Chem. Commun.* **2003**, *39*, 1606–1607; b) D. Maity, T. S. Govindaraju, *Chem. Commun.* **2012**, *48*, 1039–1041; c) S. H. Kim, H. S. Choi, J. Kim, S. J. Lee, D. T. Quang, J. S. Kim, *Org. Lett.* **2010**, *12*, 560–563; d) S. B. Maity, P. K. Bharadwaj, *Inorg. Chem.* **2013**, *52*, 1161–1163; e) S. Kim, J. Y. Noh, K. Y. Kim, J. H. Kim, H. K. Kang, S.-W. Nam, S. H. Kim, S. Park, C. Kim, J. Kim, *Inorg. Chem.* **2012**, *51*, 3597–3602.
- [5] a) L. E. Kreno, K. Leong, O. K. Farha, M. Allendorff, R. P. Van Duyne, J. T. Hupp, *Chem. Rev.* **2012**, *112*, 1105–1125; b) Y. Cui, Y. Yue, G. Qian, B. Chen, *Chem. Rev.* **2012**, *112*, 1126–1162; c) M. D. Allendorff, C. A. Bauer, R. K. Bhakta, R. J. T. Houk, *Chem. Soc. Rev.* **2009**, *38*, 1330–1352; d) W. P. Lustig, S. Mukherjee, N. D. Rudd, A. V. Desai, J. Li, S. K. Ghosh, *Chem. Soc. Rev.* **2017**, *46*, 3242–3285; e) Y. Zhang, S. Yuan, G. Day, X. Wang, X. Yang, H.-C. Zhou, *Coord. Chem. Rev.* **2018**, *354*, 28–45; f) S. Pramanik, C. Zheng, X. Zhang, T. J. Emge, J. Li, *J. Am. Chem. Soc.* **2011**, *133*, 4153–4155; g) B. Wang, X.-L. Lv, D. Feng, L.-H. Xie, J. Zhang, M. Li, Y. Xie, J.-R. Li, H.-C. Zhou, *J. Am. Chem. Soc.* **2016**, *138*, 6204–6216; h) A. Mallick, A. M. El-Zohry, O. Shekhah, J. Yin, J. Jia, H. Aggarwal, A.-H. Emwas, O. F. Mohammed, M. Eddaoudi, *J. Am. Chem. Soc.* **2019**, *141*, 7245–7249.
- [6] a) B. Chen, L. Wang, Y. Xiao, F. R. Fronczek, M. Xue, Y. Cui, G. Qian, *Angew. Chem. Int. Ed.* **2009**, *48*, 500–503; *Angew. Chem.* **2009**, *121*, 508–511; b) B. Chen, Y. Yang, F. Zapata, G. Lin, G. Qian, E. B. Lobkovsky, *Adv. Mater.* **2007**, *19*, 1693–1696; c) B. Chen, S. Xiang, G. Qian, *Acc. Chem. Res.* **2010**, *43*, 1115–1124.
- [7] a) W.-M. Chen, X.-L. Meng, G.-L. Zhuang, Z. Wang, M. Kurmoo, Q.-Q. Zhao, X.-P. Wang, B. Shan, C.-H. Tunga, D. Sun, *J. Mater. Chem. A* **2017**, *5*, 13079–13085; b) D. M. Chen, N. N. Zhang, C. S. Liu, M. Du, *J. Mater. Chem. C* **2017**, *5*, 2311–2317; c) D. K. Singha, P. Mahata, *Inorg. Chem.* **2015**, *54*, 6373–6379; d) Z. Chen, Y. Sun, L. Zhang, D. Sun, F. Liu, Q. Meng, R. Wang, D. Sun, *Chem. Commun.* **2013**, *49*, 11557–11559; e) J.-N. Hao, B. Yan, *J. Mater. Chem. C* **2014**, *2*, 6758–6764; f) H. Xu, M. Fang, C.-S. Cao, W.-Z. Qiao, B. Zhao, *Inorg. Chem.* **2016**, *55*, 4790–4794; g) C.-L. Zhang, Z.-T. Liu, H. Xu, H.-G. Zheng, J. Ma, J. Zhao, *Dalton Trans.* **2019**, *48*, 2285–2289.
- [8] A. Y. Tam, K. M. Wong, V. W. Yam, *J. Am. Chem. Soc.* **2009**, *131*, 6253–6260.
- [9] a) Special Issue on MOF: H.-C. Zhou, J. R. Long, O. M. Yaghi, *Chem. Rev.* **2012**, *112*, 673–674; b) Themed collection on MOF: J.-R. Li, R. J. Kuppler, H.-C. Zhou, *Chem. Soc. Rev.* **2009**, *38*, 1477–1504; c) H.-C. Zhou, S. Kitagawa, *Chem. Soc. Rev.* **2014**, *43*, 5415–5418; d) Q. G. Zhai, X. Bu, X. Zhao, D. S. Li, P. Feng, *Acc. Chem. Res.* **2017**, *50*, 407–417; e) M. Du, C.-P. Li, C.-S. Liu, S.-M. Fang, *Coord. Chem. Rev.* **2013**, *257*, 1282–1305; f) J.-M. Lin, C.-T. He, Y. Liu, P.-Q. Liao, D.-D. Zhou, J. P. Zhang, X.-M. Chen, *Angew. Chem. Int. Ed.* **2016**, *55*, 4674–4678; *Angew. Chem.* **2016**, *128*, 4752–4756.
- [10] a) M. C. Das, S. C. Xiang, Z. Zhang, B. Chen, *Angew. Chem. Int. Ed.* **2011**, *50*, 10510–10520; *Angew. Chem.* **2011**, *123*, 10696–10707; b) S. Henke, A. Schneemann, A. Wütscher, R. A. Fischer, *J. Am. Chem. Soc.* **2012**, *134*,

- 9464–9474; c) S. Yuan, J.-S. Qin, L. Zou, Y.-P. Chen, X. Wang, Q. Zhang, H.-C. Zhou, *J. Am. Chem. Soc.* **2016**, *138*, 6636–6642.
- [11] a) J. Zhao, Y.-N. Wang, W.-W. Dong, Y.-P. Wu, D.-S. Li, Q.-C. Zhang, *Inorg. Chem.* **2016**, *55*, 3265–3271; b) B. Wang, Q. Yang, C. Guo, Y. Sun, L.-H. Xie, J.-R. Li, *ACS Appl. Mater. Interfaces* **2017**, *9*, 10286–10295; c) Z. Xiang, C. Fang, S. Leng, D. Cao, *J. Mater. Chem. A* **2014**, *2*, 7662–7665; d) W. Liu, T. Jiao, Y. Li, Q. Liu, M. Tan, H. Wang, L. Wang, *J. Am. Chem. Soc.* **2004**, *126*, 2280–2281; e) L. Wen, X. Zheng, K. Lv, C. Wang, X. Xu, *Inorg. Chem.* **2015**, *54*, 7133–7135; f) G. Ji, J. Liu, X. Gao, W. Sun, J. Z. Wang, S. Zhao, Z. L. Liu, *J. Mater. Chem. A* **2017**, *5*, 10200–10205; g) F. Rouhani, A. Morsali, *Chem. Eur. J.* **2018**, *24*, 5529–5537.
- [12] a) W. Yan, C. Zhang, S. Chen, L. Han, H. Zheng, *ACS Appl. Mater. Interfaces* **2017**, *9*, 1629–1634.
- [13] J. An, C. M. Shade, D. A. C. Czegan, S. Petoud, N. L. Rosi, *J. Am. Chem. Soc.* **2011**, *133*, 1220–1223.
- [14] A. L. Spek, *J. Appl. Crystallogr.* **2003**, *36*, 7–13.
- [15] a) L. P. Zhang, J. F. Ma, J. Yang, Y. Y. Pang, J. C. Ma, *Inorg. Chem.* **2010**, *49*, 1535–1550; b) J. Yang, Q. Yue, G. D. Li, J. J. Cao, G. H. Li, J. S. Chen, *Inorg. Chem.* **2006**, *45*, 2857–2865.
- [16] a) L.-H. Cao, F. Shi, W.-M. Zhang, S.-Q. Zang, T. C. W. Mak, *Chem. Eur. J.* **2015**, *21*, 15705–15712; b) R. Wang, X. Liu, A. Huang, W. Wang, Z. Xiao, L. Zhang, F. Dai, D. Sun, *Inorg. Chem.* **2016**, *55*, 1782–1787; c) L. J. Han, W. Yan, S. G. Chen, Z. Z. Shi, H. G. Zheng, *Inorg. Chem.* **2017**, *56*, 2936–2940.
- [17] a) F. Yang, G. Xu, Y. Dou, B. Wang, H. Zhang, H. Wu, W. Zhou, J.-R. Li, B. Chen, *Nat. Energy* **2017**, *2*, 877–883; b) C.-R. Li, S.-L. Li, X.-M. Zhang, *Cryst. Growth Des.* **2009**, *9*, 1702–1707.
- [18] J. Huheey, E. A. Keiter, R. L. Keiter, *Inorganic Chemistry: Principles of Structure and Reactivity*, 4th ed.; Pearson Education: New York, **2000**.
- [19] a) T. Matsumoto, M. Maeda, H. Kobayashi, *Nanoscale Res. Lett.* **2016**, *11*, 7–10; b) M. Wang, L. Guo, D. Cao, *Sens. Actuators B* **2018**, *256*, 839–845.
- [20] A. Karmakar, A. V. Desai, S. K. Ghosh, *Coord. Chem. Rev.* **2016**, *307*, 313–341.

Manuscript received: May 12, 2021

Accepted manuscript online: June 10, 2021

Version of record online: July 6, 2021